Magnetoelectric and magnetoelastic properties of rare-earth ferroborates

Cite as: Low Temp. Phys. **36**, 511 (2010); https://doi.org/10.1063/1.3457390
Published Online: 20 July 2010

A. M. Kadomtseva, Yu. F. Popov, G. P. Vorob'ev, A. P. Pyatakov, S. S. Krotov, K. I. Kamilov, V. Yu. Ivanov, A. A. Mukhin, A. K. Zvezdin, A. M. Kuz'menko, L. N. Bezmaternykh, I. A. Gudim, and V. L. Temerov

Magnetoelectric and magnetoelastic properties of rare-earth ferroborates

A. M. Kadomtseva,[a] Yu. F. Popov, G. P. Vorob'ev, A. P. Pyatakov, S. S. Krotov, and K. I. Kamilov

M. V. Lomonosov Moscow State University, Vorob'evy gory, Moscow 119991, Russia

V. Yu. Ivanov, A. A. Mukhin, A. K. Zvezdin, and A. M. Kuz'menko

A. M. Prokhorov Institute of Physics of the Russian Academy of Sciences, Moscow 119991, Russia

L. N. Bezmaternykh, I. A. Gudim, and V. L. Temerov

L. V. Kirenskiĭ Institute of Physics of the Siberian Branch of the Russian Academy of Sciences, Krasnoyarsk 660036, Russia

(Submitted November 5, 2009; revised December 12, 2009)
Fiz. Nizk. Temp. **36**, 640–653 (June 2010)

The magnetic, electric, magnetoelectric, and magnetoelastic properties of rare-earth ferroborates $RFe_3(BO_3)_4$ (R=Pr, Nd, Sm, Eu, Gd, Tb, Dy, Ho, Er) as well as yttrium ferroborate $YFe_3(BO_3)_4$ have been studied comprehensively. A strong dependence not only of the magnetic but also magnetoelectric properties on the type of rare-earth ion, specifically, on its anisotropy, which determines the magnetic structure and the large contribution to the electric polarization, has been found. This is manifested in the strong temperature dependence of the polarization below the Néel point T_N and its specific field dependence, which is determined by the competition between the external and exchange *f-d* fields. A close correlation has been found between the magnetoelastic properties of ferroborates and the magnetoelastic and magnetic anomalies at magnetic-field induced phase transitions. It is found that in easy-plane ferroborates, together with magnetic-field induced electric polarization spontaneous polarization also arises below the Néel point. The ferroelectric ordering in ferroborates is of extrinsic character, giving rise to strong magnetoelectric coupling below T_N. Aside from the antiferromagnetic phase transition, the particulars of the structural phase transition accompanied by anomalies of the dielectric and magnetoelectric properties are examined for the first time. The character of the dielectric anomalies at a structural transition is analyzed for the first time on the basis of Landau's approach. © *2010 American Institute of Physics*. [doi:10.1063/1.3457390]

I. INTRODUCTION

An intensive search for new ferroelectrics has been going on over the last fifty years after the discovery and substantiation by Smolenskiĭ[1] of the phenomenon of ferroelectromagnetism (coexistence of magnetic and electric order) in certain materials.[2,3] From our standpoint, among the ferroelectromagnets discovered over this time the most interesting one is bismuth ferroborate $BiFeO_3$ ($R3c$)—a promising material with high Curie temperature (T_C=1080 K) and Néel temperature (T_N=640 K). This intrinsic ferroelectromagnet is still being studied intensively.[4,5] A distinguishing feature of $BiFeO_3$ is the absence of a center of inversion in both the crystal and the magnetic structure.

Subsequent searches for new ferroelectromagnets have led to the discovery of magnetoelectric properties in rare-earth magnets $RMnO_3$ ($Pbnm$), in which electric polarization arises with cycloidal magnetic ordering, which destroys the inversion symmetry (extrinsic ferroelectrics). The appearance of spontaneous electric polarization in the system $RMnO_3$ depends largely on the ionic radius of the rare-earth ion and is observed only in manganites with a small ionic radius (Gd, Tb, Dy) and some substituted compositions.[6–11] The magnetoelectric effects are manifested most strongly in such systems, and a magnetic field can directly affect the orientation of the electric polarization, which creates the prerequisites for practical applications of these materials.

In the 1990s Schmid introduced a new term—multiferroics—for materials in which at least two of three parameters—magnetic, electric, and elastic—are present simultaneously.[12] This term has essentially replaced the term ferroelectromagnetic.[1]

In recent years a new class of multiferroics has been discovered—rare-earth ferroborates $RFe_3(BO_3)_4$, which possess a noncentrosymmetric space group ($R32$). Magnetoelectric interactions manifest in them as anomalies in the magnetic field dependences of the electric polarization with changes of the magnetic structure of the iron subsystems.[13,14]

The diversity of the properties of ferroborates (see, for example, Refs. 15 and 16) is due to the presence in them of two magnetic subsystems: iron ions and rare-earth ions.

The crystal structure of the ferroborates is such that direct Fe–Fe exchange in the system dominates and is much stronger than indirect exchange between ions of rare-earth elements, occurring by the path R–O–B–O–R.[17] This is indicated by, specifically, the closeness of the Néel temperature in ferroborates with different rare earths. This gives a basis for assuming that the rare-earth ions are subject mainly to the effect of the exchange field of the Fe subsystem and the external magnetic field, which induce magnetic order in the R subsystem, as is confirmed by measurements of the mag-

TABLE I. Properties of rare-earth ferroborates $RFe_3(BO_3)4$.

R	R_{ion}, A	T_s, K	T_N, K	Δ, cm^{-1}	anisotropy $g_\parallel/g_\perp$, T_{sr}
Pr	0.99	—	32		↑
Nd	0.98	—	31	8.8	→ 1.4/2.4
Sm		—	31		→
Eu	0.95	88	34		→
Gd	0.94	174	37	6.9	↑→ 10 K
Tb	0.92	241	41	32	↑ 18/0
Dy	0.91	340	39	16.7	↑ 15/7
Ho	0.89	427	39		↑→ 5 K
Er		450?	39	7.3	→ 1.3/9
Y	0.89	445	38		—

Note: R—rare-earth ion, T_s—structural transition temperature, T_N—antiferromagnetic ordering temperature, T_{sr}—spin-reorientation temperature, horizontal and vertical arrows designate easy-plane and easy-axis anisotropy, respectively; Δ—Zeeman splitting of the levels in the ground state. The data are taken from Ref. 16.

netization and temperature dependences of the magnetic susceptibility for ferroborates.[18–20] The appearance of order in the rare-earth system below the Néel temperature, observed in Tb ferroborate[21] and Ho ferroborate,[22] is of an induced character and is caused by the *f-d* exchange field of the order of tens of kilo-oersteds, acting in the R subsystem from the side of the iron ions.

The weakness of the exchange interactions in the rare-earth subsystem does not mean that the role of the rare earth is negligible. The orientation of the magnetic moments of the iron ions relative to the crystallographic axes is determined by the type of rare-earth ion: either easy-axis antiferromagnetic structure, when the iron spins are oriented along the trigonal axis *c* (R=Dy, Tb, Pr),[19–22] or and easy-plane structure (R+Nd, Eu, Er), when the iron spins are oriented in the *ab* plane perpendicular to the *c* axis of the crystal.[14,18,23–29]

In the present work we examine the effect of the type of rare-earth ion and its ground state in a crystal field on the magnetic and magnetoelectric properties of ferroborates. Anomalies of the dielectric properties at structural and antiferromagnetic phase transitions are also examined.

II. CRYSTAL AND MAGNETIC SYMMETRY OF RARE-EARTH FERROBORATES

A. Structural phase transition

At high temperatures all crystals in the $RFe_3(BO_3)_4$ family possess trigonal structure, which belongs to the space group *R*32. In compounds with a large ionic radius (*R*=La, Ce, Pr, Nd, Sm) this structure remains unchanged down to the lowest temperatures, while in compounds with a shorter ionic radius (R=Eu, Gd, Tb, Dy, Ho, Er) a structural phase transition occurs at a temperature that increases (see Table I) with decreasing ionic radius.[30,31]

A structural transition is accompanied by anomalies of the dielectric properties (Fig. 1a) and thermal expansion (Fig. 1b). A transition into a low-symmetry phase is also accompanied by anomalies of the magnetoelectric properties,

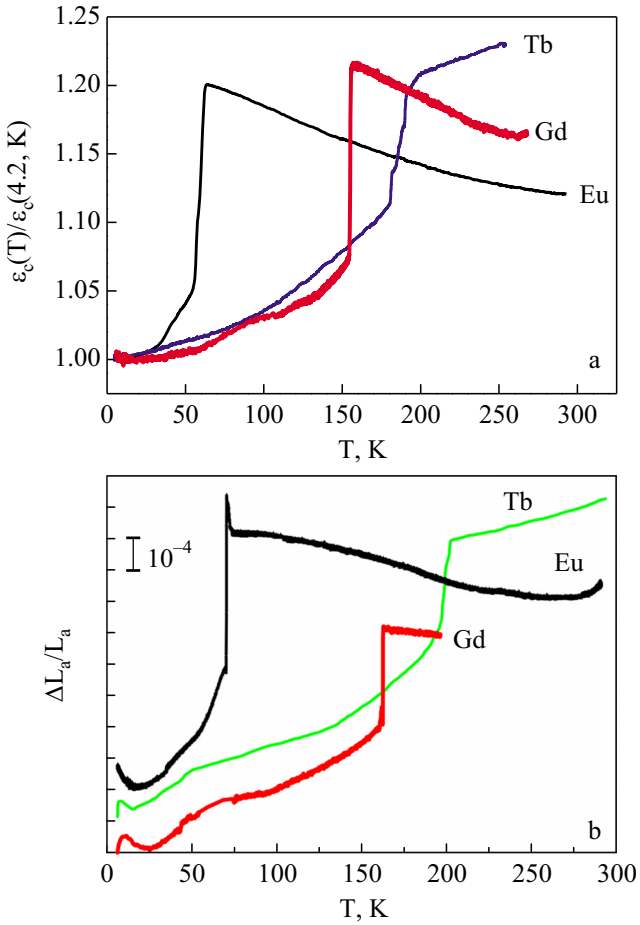

FIG. 1. Temperature dependences of the permittivity (a) and thermal expansion (b) for Eu, Gd, Tb ferroborates.

which can be seen from the temperature dependence of the magnetically induced electric polarization for $EuFe_3(BO_3)_4$, in which an appreciable change of the polarization was observed at the point of a structural phase transition at $T_s \sim 70$ K (Fig. 2).

We shall now examine this structural phase transition. The change of the space symmetry group at the transition $R32 \rightarrow P3_121$ (Ref. 17) signifies that the crystal class of the system D_3 (determined by its rotational symmetry elements)

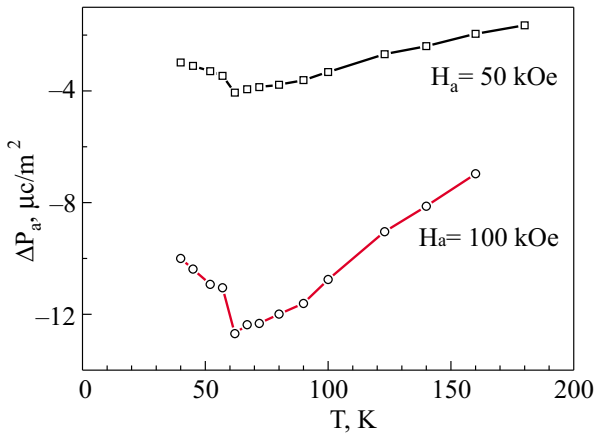

FIG. 2. Anomaly in the temperature dependence of the longitudinal electric polarization along the *a* axis for $EuFe_3(BO_3)_4$ at a structural phase transition.

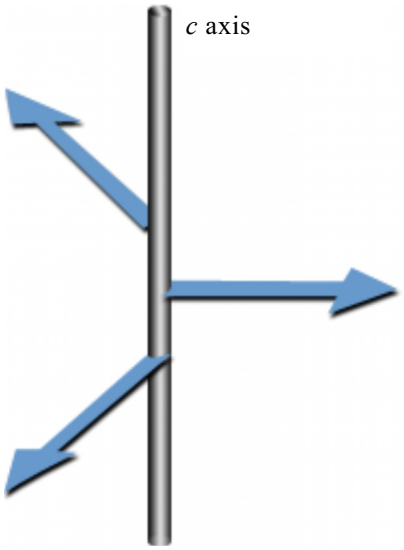

FIG. 3. Helicoidal antiferroelectric structure, hypothetically established at temperature $T<T_s$.

remains unchanged (the macrosymmetry of the system does not change) but certain spatial translations are lost, which is characteristic for antiferroelectric phase transitions. The volume of the primitive cell of a rare-earth ferroborate crystal adjusts, and the primitive cell of the new space group becomes hexagonal (the primitive cell of the initial space group $R32$ was rhombohedral).

To simplify the analysis (but preserve the characteristic, in terms of the change of symmetry, behavior of our system), in constructing the structural order parameter we shall focus our attention on taking account of the displacements of the R^{3+} ions only. In the general case the order parameter will be proportional to a linear combination of the displacements of all ions of the system for the corresponding vibrational mode, but in a phenomenological study taking account of only the symmetry properties of the order parameter such concretization is immaterial.

The R^{3+} ions with charge q which are displaced as a result of a structural phase transition form a helicoidal wave, spontaneously appearing in the system, of electric polarization density:

$$\delta\mathbf{P} = \sum_i q\Delta[\mathbf{n}_1 \cos(\mathbf{k}\cdot\mathbf{r}_i) + \mathbf{n}_2 \sin(\mathbf{k}\cdot\mathbf{r}_i)], \quad (1)$$

where $\mathbf{n}_1$ and $\mathbf{n}_2$ are mutually perpendicular unit vectors lying in the horizontal plane; the vector $\mathbf{n}_1$ is directed along the displacements of the R^{3+} ions from the atomic layer passing through the origin of coordinates, Δ is the magnitude of the corresponding spontaneous displacements of the ions, k is the wave vector of the helicoid, oriented along the c axis and commensurate to the lattice constant ($|\mathbf{k}|=2\pi/c$).

Thus it can be assumed that as a result of a structural phase transition at temperature T_s our system becomes a noncollinear antiferromagnet of the helicoidal type, and the electric structure arising does not result in a change of the crystal class of the system (Fig. 3). Its macrosymmetry is characterized once again by the group 32 (such phase transitions are said to be isomorphic), which is a characteristic property of a transition at the point T_s. This makes it possible to explain the dielectric anomalies observed at the transition through the point T_s (Fig. 1a), specifically, the different magnitude of the changes along the c axis and in the basal plane, as being due to the transverse nature of the wave of electric polarization (see Fig. 3). Likewise it can be shown (see Appendix) that at the structural phase transition point T_s the electric susceptibility in the basal plane undergoes a jump, whose magnitude is proportional to the squared antiferroelectric order parameter Δ. Hence it follows that there is no divergence at the phase transition point (the susceptibility does not conform to the Curie–Weiss law).

B. Magnetic structure below the antiferromagnetic phase transition

Antiferromagnetic ordering arising below T_N doubles the unit cell along the c axis, and the magnetic unit cell ferroborate no longer coincides with the crystallochemical cell. This complicating circumstance distinguishes the material under consideration from the typical objects in the symmetry theorem of antiferromagnetism,[32] where it is assume that the cells do coincide. An obvious way to overcome this difficulty is to double the crystallochemical cell of ferroborate and thereby return to the conventional approach, studying the reduced space group $R32$, in which translations by the unit-cell constants in the basal plane and double translation along the c axis are assumed to be equal to the identity transformation. Following this approach, in Ref. 14 the following relations were obtained from a symmetry analysis for the components of the electric polarization vector $\mathbf{P}$ of ferroborate:

$$P_x = c_1 L_y L_z + c_2(L_x^2 - L_y^2) + \frac{1}{2}\sum_{i=1}^{2}[c_3(m_{ix}^2 - m_{iy}^2) + c_5 m_{iz} m_{iy}], \quad (2a)$$

$$P_y = -c_1 L_x L_z - 2c_2 L_x L_y - \frac{1}{2}\sum_{i=1}^{2}(2c_3 m_{ix} m_{iy} + c_5 m_{iz} m_{ix}), \quad (2b)$$

$$P_z = c_6 L_x L_z (L_x^2 - 3L_y^2) + \frac{1}{2}c_7 \sum_{i=1}^{2} m_{ix} m_{iz}(m_{ix}^2 - 3m_{iy}^2), \quad (2c)$$

where $\mathbf{L}$ is the antiferromagnetic order parameter for the Fe^{3+} ions, $\mathbf{m}_i$ are the magnetic moments of rare-earth ions, the summation extends over two paramagnetic "sublattices," $i=1, 2$ into which the rare-earth subsystem is divided as a result of the antiferromagnetic ordering of the iron ions.

Similarly, we obtain for the longitudinal components of the magnetostriction

$$u_{xx} - u_{yy} = b_1 L_y L_z + b_2(L_x^2 - L_y^2) + \frac{1}{2}\sum_{i=1}^{2}[b_3(m_{ix}^2 - m_{iy}^2) + b_4 m_{iz} m_{iy}], \quad (3a)$$

$$u_{zz} = b_5(L_x^2 + L_y^2) + b_6 L_z^2 + \frac{1}{2}\sum_{i=1}^{2}[b_7(m_{ix}^2 + m_{iy}^2) + b_8 m_{iz}^2]. \quad (3b)$$

The coefficients c_i and b_i in Eqs. (2) and (3) are identical for both rare-earth "sublattices." This is explained by the fact that all rare-earth ions occupy the same crystallographic position and differ only by the exchange field acting on them.

As a result of a structural phase transition with tripling of the unit-cell volume the total number of magnetically active Fe^{3+} ions per unit cell becomes equal to nine. In addition, these nine ions are divided into two nonequivalent subsystems, which in turn consist of three and six magnetic ions—in accordance with the types of symmetry of the sites occupied by the iron ions in the new crystal symmetry of the system. As follows from the experimental data,[33] collinear antiferromagnetic ordering arises at temperature T_N. It can be shown[34] that the order parameter of the indicated magnetic order in the exchange approximation will be one-dimensional and will be the sum of the order parameters of the antiferromagnetic order of each subsystem of the Fe^{3+} ions (consisting of, respectively, three and six ions per unit cell). With respect to its conventional properties (relative to the generators of the point transformations 3 and 2 present in the space group $P3_121$) this order parameter will be equivalent to the antiferromagnetic order parameter for $R32$ symmetry). On this basis the collinear antiferromagnetic ordering of the magnetic sublattice of iron ions will be characterized by a general antiferromagnetism vector **L** and the relations (2) and (3) will remain unchanged.

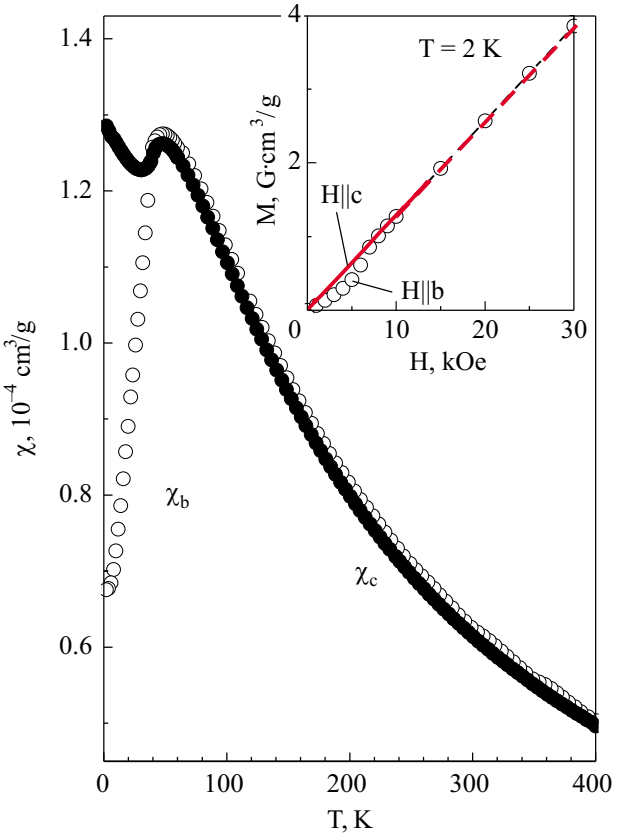

FIG. 4. Temperature dependences of the magnetic susceptibility along (χ_e) and perpendicular (χ_b) to the c axis in $YFe_3(BO_3)_4$, measured in the field 1 kOe. Inset: curves of the magnetization perpendicular and parallel to the c axis.

III. MAGNETIC, MAGNETOELECTRIC, AND MAGNETOELASTIC PROPERTIES OF FERROBORATES WITH DIFFERENT TYPES OF RARE-EARTH ION

A. Magnetic properties of ferroborates. Effect of rare-earth ions

As noted above, the magnetic properties of ferroborates depend strongly on the type of rare-earth ion, its ground state in the crystal, and the exchange (R–Fe) fields, which determine the contribution to the magnetization and anisotropy of the system.

We shall examine first the properties of $YFe_3(BO_3)_4$, where the rare-earth contribution is zero. Figure 4 shows the temperature dependence of the magnetic susceptibility along and perpendicular to the trigonal axis c, respectively. The susceptibility in the paramagnetic region is isotropic and conforms to the Curie–Weiss law: $\chi_{Fe}(T)=C_{Fe}/(T+\theta_{Fe})$ where the Curie paramagnetic temperature $\theta_{Fe}\approx 130$ K and the Curie constant C_{Fe} is close to its theoretical value. At temperatures $T<T_N\approx 38$ K the susceptibility becomes anisotropic: it decreases sharply in the basal plane, while along the c axis it varies negligibly and practically retains its value at the Néel point. Such behavior of the susceptibility indicates that the Fe^{3+} spins become ordered in the basal plane, and the finite value of the susceptibility in this plane is due to the fact that there exists a distribution of easy axes, which is determined either by the natural trigonal anisotropy or induced by magnetoelastic anisotropy. The application of a weak magnetic field in the plane turns the spins perpendicular to the field, which is manifested in a small nonlinearity of the magnetization curves, after which the magnetization in the basal plane increases linearly with the field (and practically coincides with the magnetization $M_c(H_c)$ along the c axis), determining the transverse susceptibility $\chi_\perp^{Fe}\approx 0.125\cdot 10^{-3}$ cm^3/g (see inset in Fig. 4).

We now turn to the easy-plane ferroborates with magnetic rare-earth ions. We shall examine the behavior of $EuFe_3(BO_s)_4$ in which the magnetism of the Eu^{3+} ion is of a van Vleck character. Figure 5 shows the temperature dependences of the susceptibility, which even in the paramagnetic region manifest anisotropy ($\chi_\perp>\chi_c$) evidently associated with an anisotropic van Vleck contribution of the Eu subsystem: $\chi_{c,\perp}=\chi_{Fe}+\chi_{c,\perp}^{VV}$, where $\chi_\perp^{VV}>\chi_c^{VV}$. In the region of antiferromagnetic ordering at $T<T_N$ the anisotropy of the susceptibility increases as a result of the Fe subsystem, whose spins lie in the basal plane. In a magnetic field $H>6$ kOe applied in this plane the Fe^{3+} spins become reoriented perpendicular to the field, as one can see from the magnetization curves in the inset in Fig. 5. This increases the susceptibility $\chi_\perp=\chi_b$ (curve at 10 kOe in Fig. 5), which, however, remains less than χ_c, in contrast to $YFe_3(BO_3)_4$, because of the van Vleck contribution, which is practically temperature-independent below 100 K.

We shall now examine the easy-plane ferroborate $ErFe_3(BO_3)_4$, in which the anisotropic properties of the rare-earth subsystem are even more clearly manifested. Figure 6a shows the temperature dependences of the magnetic susceptibility along and perpendicular to the c axis, whose strong anisotropy ($\chi_\perp>\chi_c$), associated with the contribution of the Er^{+3} ions, is manifested even at high temperatures and increases substantially with decreasing temperature. At low

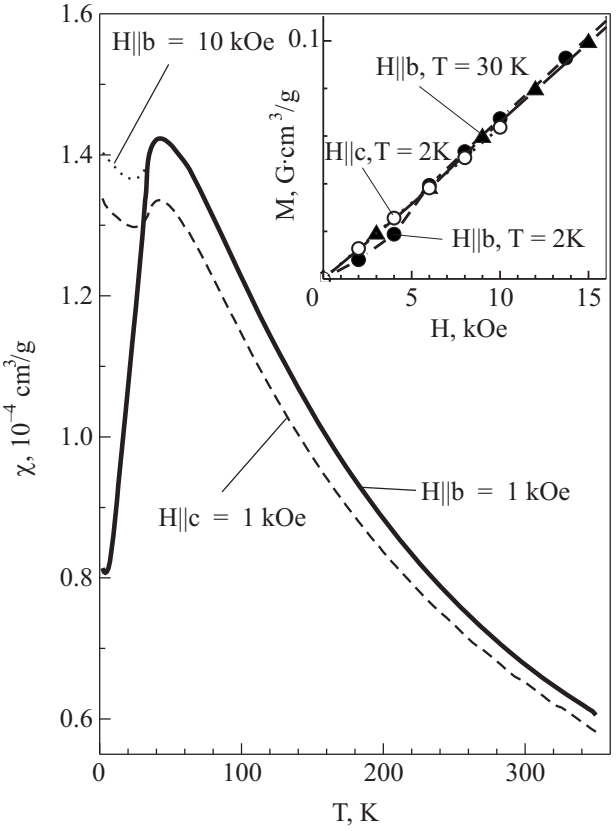

FIG. 5. Temperature dependences of the magnetic susceptibility parallel (**H**∥**c**) and perpendicular (**H**∥**b**) to the c axis in $EuFe_3(BO_3)_4$, measured in field 1 and 10 kOe. Inset: curves of the magnetization perpendicular and parallel to the c axis.

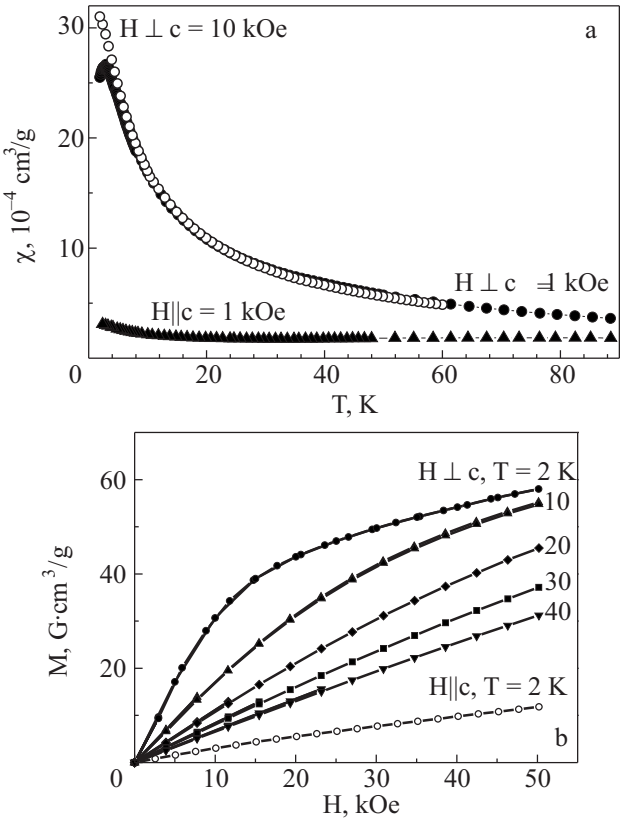

FIG. 6. Temperature dependences of the magnetic susceptibility parallel and perpendicular to the c axis in $ErFe_3(BO_3)_4$, measured in fields 1 and 10 kOe (a).Curves of the magnetization of $ErFe_3(BO3)_4$ perpendicular and parallel to the c axis (b).

temperatures the bottom Kramers doublet of Er^{+3}, whose g-tensor, as follows from these data, has a strong anisotropy ($g_\perp \gg g_c$), makes a strong contribution to the magnetic properties. This is confirmed by the magnetization curves $M_\perp(H_\perp)$ (Fig. 6b), which has a characteristic low-temperature kink associated with saturation of the contribution of the main doublet, and the linearity of the dependence $M_c(H_c)$ indicates that the c component of g tensor is small. The existence of the low-temperature maximum in the temperature dependence of the susceptibility in the basal plane (Fig. 6a, curve for $H=1$ kOe) is due to the decrease of the longitudinal part of the susceptibility of the Er subsystem, antiferromagnetically polarized by the exchange field of the Fe^{3+} spins lying in the ab plane. When a 10 kOe magnetic field is applied, which reorients the Fe^{3+} spins and magnetic moments of Er^{3+} perpendicular to the field, this feature in the susceptibility vanishes, and it increases monotonically right down to the lowest temperatures (Fig. 6a, curve for $H=10$ kOe).

Magnetic properties qualitatively different from $ErFe_3(BO_3)_4$ are observed in a different easy-plane ferroborate $SmFe_3(BO_3)_4$, likewise containing Kramers ions (Sm^{3+}). Figure 7 displays the temperature dependences of the magnetic susceptibility and magnetization curves demonstrating virtually complete similarity with the corresponding curves for $YFe_3(BO_3)_4$ (see above). This indicates an anomalously small magnetic contribution of Sm^{3+} ions, which is due to a characteristic feature of their ground state multiplet $^6H_{5/2}$ that is associated with the small Landé factor $g_J=2.7$. As a result, the Zeeman effect of a magnetic field on the ground state multiplet $\hat{H}=\mu_B g_J \mathbf{J}_R \cdot \mathbf{H}$ is considerably weakened. At the same time this feature of the ground-state multiplet of Sm^{3+} has no effect on the magnitude of the isotropic R–Fe exchange interaction determined by the spins of the rare-earth ion $\mathbf{S}_R$ and the iron ion $\mathbf{S}_{Fe}$: $\hat{H}^{exch}_{R-Fe}=I\mathbf{S}_R \cdot \mathbf{S}_{Fe}$, where I is the exchange integral.

In the easy-plane ferroborate $NdFe_3(BO_3)_4$ the contribution of the Nd subsystem to the anisotropic magnetic properties is smaller than in erbium ferroborate but appreciably larger than in $SmFe_3(BO_3)_4$.[26,27]

We now turn to the easy-axis ferroborates, in which the spins of the Fe^{3+} ions lie along the trigonal axis c. This state is realized in ferroborates with R=Pr,[25] Tb,[21,24] Dy,[19] and Ho,[20,22] and evidently it is stabilized as a result of the contribution of the rare-earth subsystem to the effective magnetic anisotropy energy of the crystal, since the Fe subsystem anisotropy energy itself stabilizes the easy-plane phase. At high temperatures, above the exchange (R–Fe) splitting of the bottom doublets (quasidoublets) of the rare-earth ions, the anisotropy energy $\Phi_A=K_{eff}L_z^2/2$ is determined by the effective constant $K_{eff}=K_{Fe}-\chi_c^R(H_{f-d}^c)^2+\chi_\perp^R(H_{f-d}^\perp)^2$, where $\chi_{c,\perp}^R$ and $H_{f-d}^{c,\perp}$ are, respectively, the magnetic susceptibility of the rare-earth subsystem and the effective $f-d$ exchange field along and perpendicular to the c axis. Since isotropic exchange ($H_{f-d}\approx -I(g_J-1)S_{Fe}/g_J\mu_B$) makes the main contribution to the $f-d$ interaction, the sign of the rare-earth contribution to K_{eff} is determined by the anisotropy of the magnetic susceptibility of the R ions. At low temperatures,

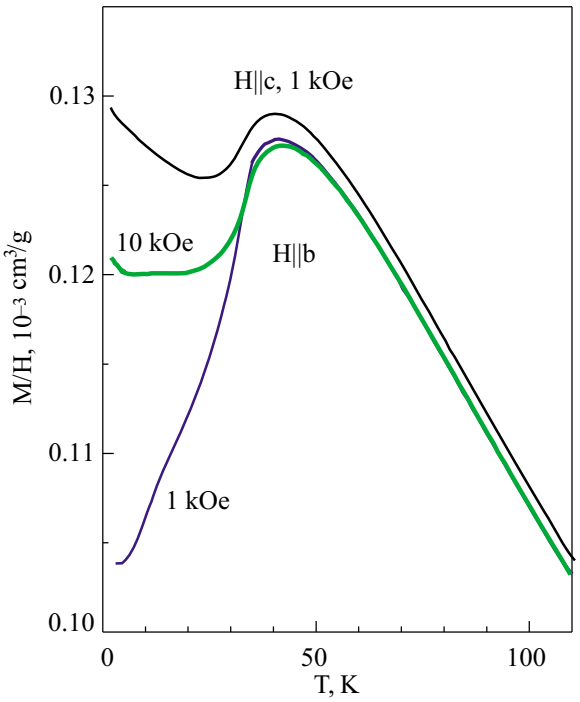

FIG. 7. Temperature dependences of the magnetic susceptibility parallel (**H**∥**c**) and perpendicular (**H**∥**b**) to the c axis in $SmFe_3(BO_3)_4$, measured in field 1 and 10 kOe.

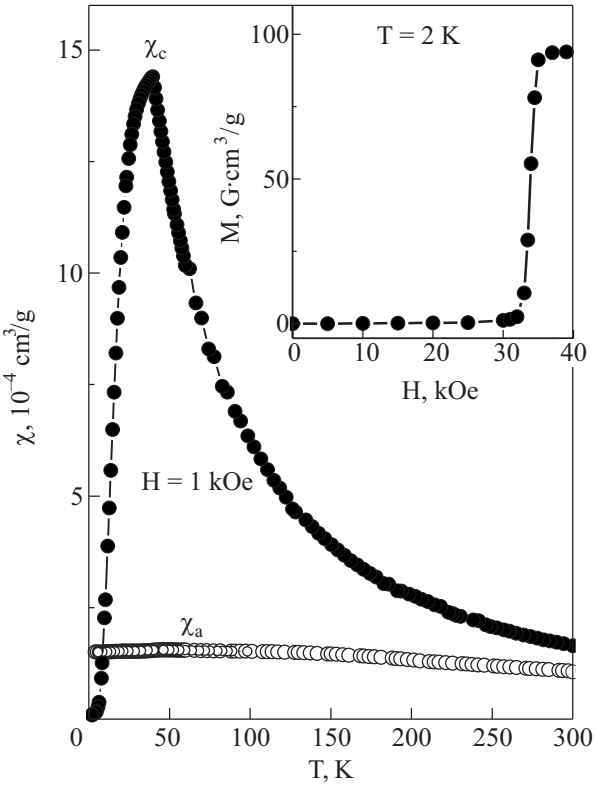

FIG. 9. Temperature dependences of the magnetic susceptibility parallel (χ_c) and perpendicular (χ_a) to the c axis in $TbFe_3(BO_3)_4$, measured in field 1 kOe. Inset: curve of the magnetization along the c axis, illustrating a spin-flop transition.

when $k_BT < \Delta_R$ and the high-temperature approximation does not work, the anisotropic contribution of the rare-earth subsystem is determined directly by the exchange splitting Δ_R of the ground state (doublet) of the rare-earth ion.

Figures 8 and 9 display the temperature dependences of the magnetic susceptibility for $PrFe_3(BO_3)_4$ and $TbFe_3(BO_3)_4$. Both ferroborates show even the paramagnetic region a substantial anisotropy of the magnetic susceptibility ($\chi_c > \chi_\perp$), stabilizing the uniaxial state. The decrease of the susceptibility χ_c observed below T_N indicates that the spins of the Fe^{3+} ions are ordered along the c axis, giving rise to antiferromagnetic polarization of the Pr^{3+} and Tb^{3+} ions as a result of the exchange interaction. A magnetic field along the c axis gives rise in both ferroborates to a spin-flop transition of the Fe^{3+} spins in the basal plane, accompanied by a jump of the magnetization (see, for example, inset in Fig. 9). For these ferroborates there are appreciable differences in the magnetization curves due to the special features of the ground state of these substances in a crystal field. In $PrFe_3(BO_3)_4$ the ground state of the Pr^{3+} ion is a singlet,[23,35] separated by ~50–60 K from the nearest excited states, while in $TbFe_3(BO_3)_4$ the ground state of the Tb^{3+} ion is a quasidoublet, split practically by the exchange field only. For this reason the field of a spin-flop transition in $TbFe_3(BO_3)_4$ at low temperatures is close to the exchange splitting field: $H_{xf} \approx \Delta^Z_{Tb}/\mu^Z_{Tb} \approx 35$ kOe, where $\mu^Z_{Tb} \approx (8.6–8,8)\mu_B$, i.e., flipping of the spins of the iron ions occurs near the magnetization reversal field of the Tb sublattice, directed opposite to the external field.

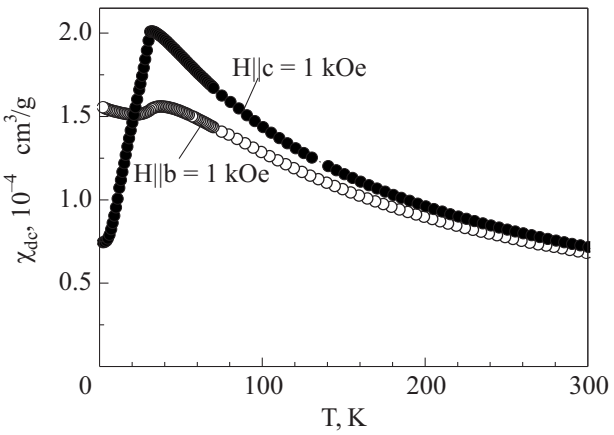

FIG. 8. Temperature dependences of the magnetic susceptibility parallel (**H**∥**c**) and perpendicular (**H**∥**b**) to the c axis in $PrFe_3(BO_3)_4$, measured in field 1 kOe.

B. Contributions of the rare-earth ion and iron ion subsystems to the magnetoelectric and magnetoelastic properties of ferroborates

To study the effect of the type of rare-earth ion on the magnetoelectric and magnetoelastic properties of ferroborates one must know how to separate the rare-earth contribution from the background due to the subsystem of iron ions. For this reason, yttrium borate $YFe_3(BO_3)_4$ was taken as a model object. In this borate there is only one magnetic subsystem—the iron ions, characterized by the order parameter **L**. In the relations (2) and (3) the magnetization components of rare-earth ions are assumed to be zero: $m_{ix} = m_{iy} = m_z = 0$. Taking account of the easy-plane anisotropy of yt-

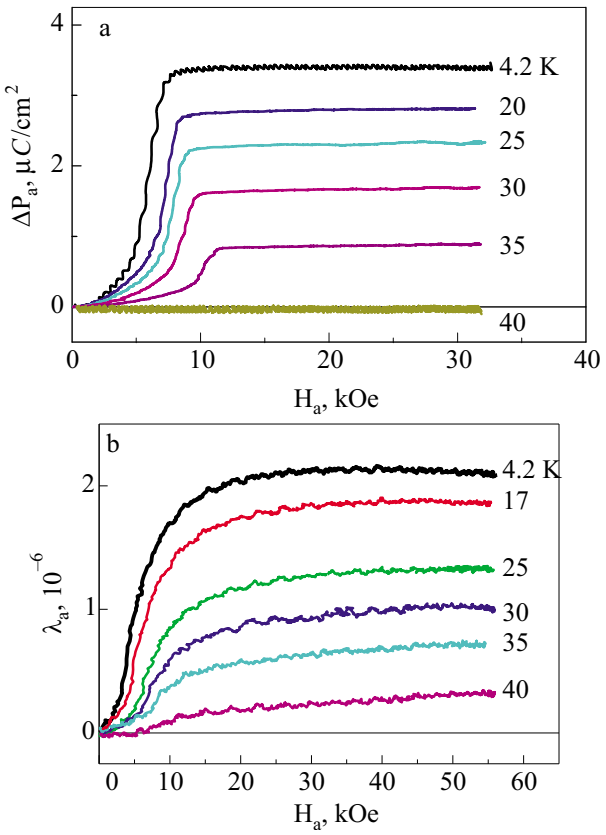

FIG. 10. Field dependences of the polarization (a) and magnetostriction (b) for yttrium ferroborate $YFe_3(BO_3)_4$, measured along the *a* axis of a crystal at different temperatures.

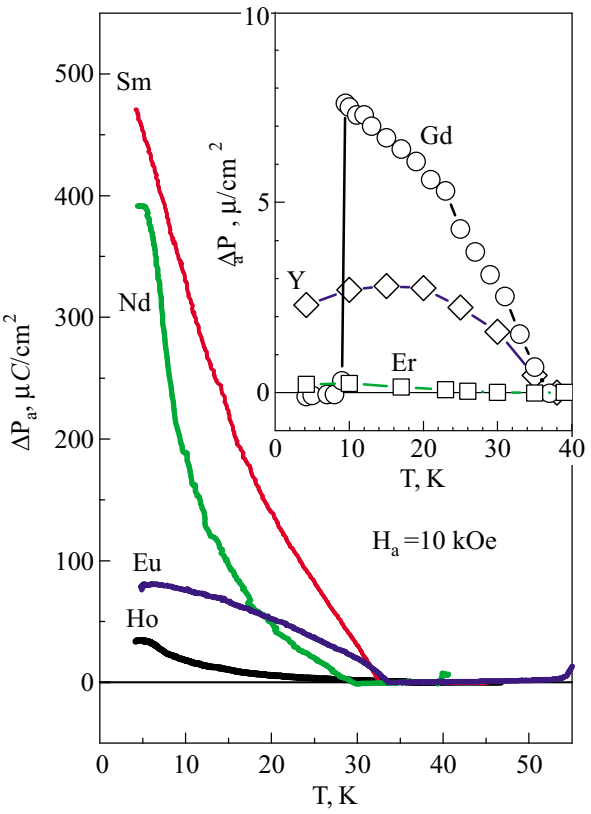

FIG. 11. Temperature dependences of the polarization along the *a* axis for easy-plane ferroborates R=Sm,Nd,Eu,Ho. Inset: dependences for ferroborates with R=Er,Gd as compared with yttrium ferroborate.

trium ferroborate $L_z=0$ the polarization and magnetostriction components in the plane are proportional to the products of L_x and L_y:

$$(P_a,P_b) \sim (L_x^2 - L_y^2; L_xL_y), \quad (u_{xx} - u_{yy}) \sim (L_x^2 - L_y^2).$$

The ratio of the components of the antiferromagnetic vector in the plane changes with reorientation of the antiferromagnetism vector **L** under the action of a magnetic field, and anomalies which are correlated with one another should be observed in the magnetoelectric and magnetoelastic dependences, which is confirmed experimentally (Fig. 10). The characteristic magnitudes of the polarization jumps are about 3 $\mu C/m^2$.

As one can see from the plots of the temperature dependences of the electric polarization $\Delta P_a(T)$ induced by the magnetic field $H_a=10$ kOe (Fig. 11), when the yttrium ions are replaced with rare-earth elements the magnitude of the polarization for a number of rare-earth ferroborates can be an order of magnitude greater than in $YFe_3(BO_3)_4$, which, evidently, is due to the appearance of terms containing nonzero components of the magnetization of the R ions $m_{i\alpha}$ in Eq. (2). Just as in $YFe_3(BO_3)_4$, a correlation is observed between the magnetoelectric and magnetoelastic properties in rare-earth ferroborates, but the magnitude of the magnetostriction does not depend so strongly on the type of rare-earth ion as the electric polarization. The latter circumstance agrees with measurements of the elastic moduli and sound speed in a terbium ferroborate single crystal,[36] which show that the observed features of the acoustic properties are due not to the magnetic single-ion anisotropy of rare-earth ions but rather the exchange interactions in the iron subsystem.

C. Relation between the rare-earth ion anisotropy and the magnitude of the magnetoelectric effects in ferroborates

As follows from the relations (2) and (3), rare-earth ion anisotropy plays a decisive role in the magnetic and magnetoelectric properties of rare-earth ferroborates. Thus, for gadolinium ferroborate with an isotropic *S* ion below T_N the magnitude of the electric polarization was small and close to that observed for $YFe_3(BO_3)_4$ (Fig. 11), since the gadolinium ions are in the *S* state ($^8S_{7/2}$) and the coupling with the crystal lattice is weak.

For easy-plane neodymium and samarium ferroborates, the electric polarization arising in magnetic fields had the maximum value for ferroborates and reached $\sim$500 $\mu C/m^2$ (Fig. 11). The electric polarization for Eu and Ho ions ($T>5$ K), which also have an easy-plane anisotropy, reaches lower but still substantial magnitudes of the order of tens of $\mu C/m^2$.

For strongly anisotropic ions (Pr, Tb, Dy) as well as Ho ($T<5$ K) an easy-axis magnetic structure is realized and the spins of the Fe^{3+} ions become ordered below T_N along the trigonal *c* axis of the crystal, giving rise to antiferromagnetic polarization of the rare-earth ions due to $f-d$ exchange. For uniaxial crystals, for example, $PrFe_3(BO_3)_4$, sharp jumps accompanied by magnetization of the rare-earth ions and flipping of the Fe^{3+} spins into the basal plane are observed in the magnetization curves in the case $\mathbf{H}\|\mathbf{c}$ (Fig. 12a). The mag-

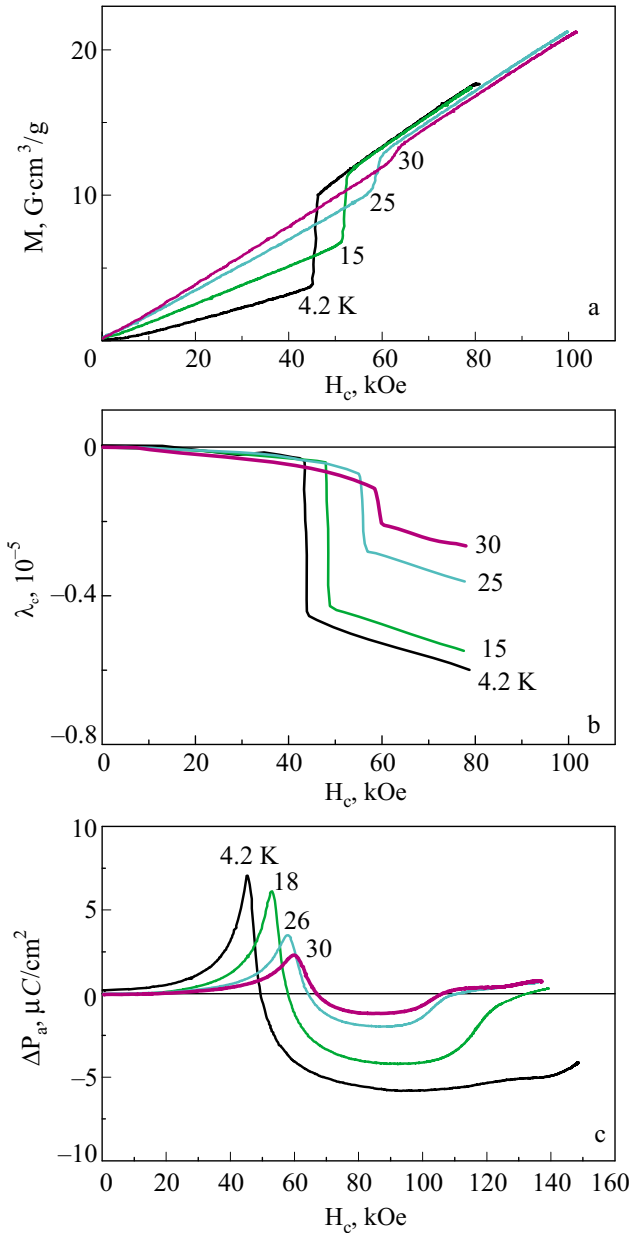

FIG. 12. Field dependences (**H**‖**c**) for the magnetization (a), magnetostriction (b), magnetically induced electric polarization (c) of $PrFe_3(BO_3)_4$ at different temperatures.

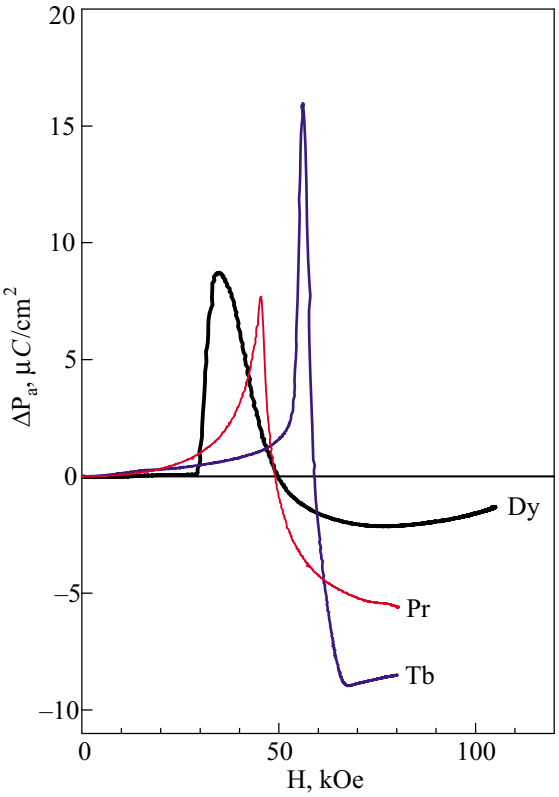

FIG. 13. Electric polarization along the *a* axis versus the magnetic field applied along the *c* axis for Dy, Pr, Tb ferroborate crystals at 4.2 K.

netic field induced phase transition of the spin-flop type is likewise accompanied by anomalies of the magnetoelastic (Fig. 12b) and magnetoelectric (Fig. 12c) properties. We note that the jumps of the electric polarization do not exceed $\sim 10\ \mu C/m^2$ (Fig. 13) and are close to those observed for the Fe subsystem; this is due to the vanishing of the rare-earth contributions to the polarization with components in the basal plane $m_{ix}=m_{iy}=0$, even though the magnetic moment $m=m_z$ is large (see Eq. (2)).

D. Manifestation of *f–d* exchange field in the field dependences of the magnetoelectric polarization

Aside from the magnitudes of the magnetically induced polarization, the magnetic-field dependences of the magnetoelectric and magnetoelastic characteristics are also of interest, since the symmetry and magnetic properties of the compounds are manifested in them.

The field dependences of the polarization in neodymium and samarium ferroborate are characteristic (Fig. 14). Substantial changes of the electric polarization, similar to those observed in yttrium ferroborate (Fig. 10a) but substantially greater in magnitude, are observed in relatively weak fields (<10 kOe); this is explained by the additional contribution of terms including the magnetic moments of the rare-earth ions $\mathbf{m}_i$ to the polarization.

These anomalies are related with the establishment of a uniform antiferromagnetic order, differing from the initial nonuniform state in which the volume averages of the polarization must be zero, in the entire volume of the crystal. The initial nonuniform state could be related with the presence of antiferromagnetic domains and with the spatially modulated structures along the *c* axis; the existence of such structures has been established for gadolinium ferroborate[37] and neodymium ferroborate.[23]

The next characteristic feature inherent to all ferroborates with easy-plane anisotropy is that the sign of the longitudinal electric polarization $P_a(H_a)$ is different from that of the transverse electric polarization $P_a(H_b)$ (Fig. 14). This follows directly from a symmetry analysis: the expression for the components of the electric polarization P_a (2a) contains the quantities $(L_x^2-L_y^2)$ and $(m_{ixi}^2-m_{iy}^2)$, whose sign changes when the magnetic field rotates by 90 degrees.

As one can see in Fig. 14, the magnetoelectric dependences of the neodymium and samarium ferroborates together with the similarity of their behavior in weak fields exhibit substantial differences for higher values of the magnetic field. In samarium ferroborate the polarization saturates in fields below 10 kOe, remaining unchanged up to the high-

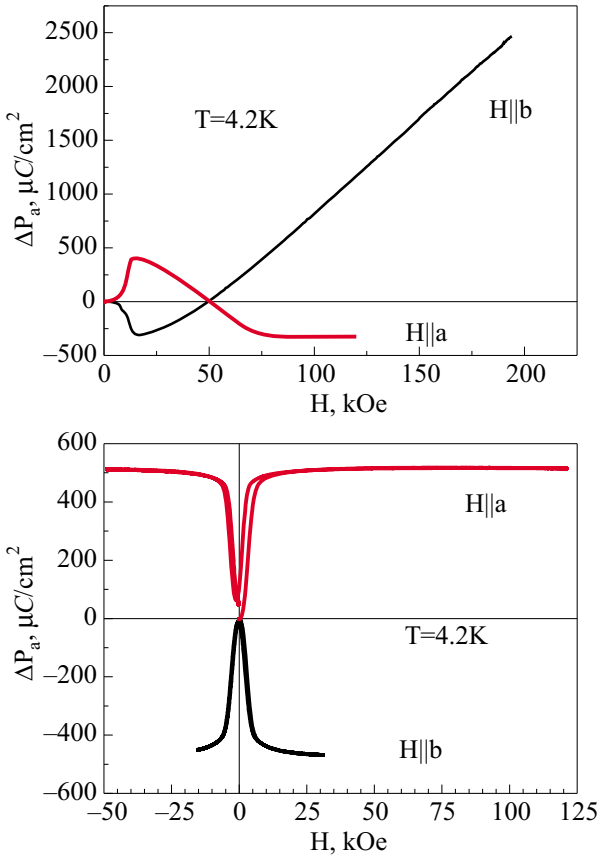

FIG. 14. Electric polarization along the *a* axis in magnetic fields **H**∥**b** and **H**∥**a** for neodymium ferroborate $NdFe_3(BO_3)_4$ (a) and samarium ferroborate $SmFe_3(BO_3)_4$ (b).

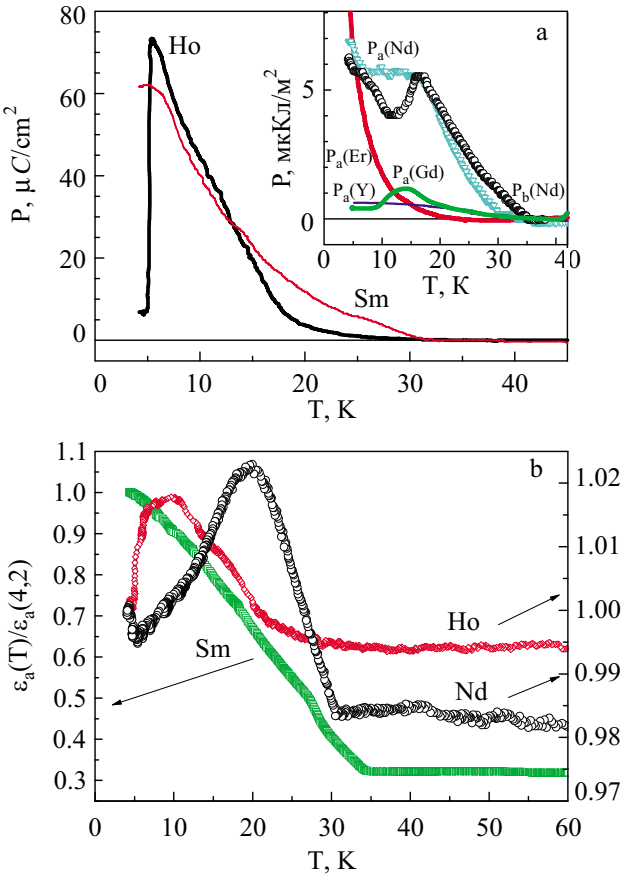

FIG. 15. Temperature dependence of the spontaneous polarization of ferroborates with different rare-earth ions (a). Inset: temperature dependences for Er, Gd, Y ferroborates and Nd ferroborate alon the *a* and *b* axes. The temperature dependence of the permittivity for Sm, Nd, Ho ferroborates (b).

est fields attainable experimentally, while in neodymium ferroborate the polarization changes sign in fields ~50 kOe. We have observed a similar sign-change of the polarization in holmium ferroborate in weaker fields (15–20 kOe). As shown in Ref. 14 this phenomenon can be explained on the basis of a model in which the rare-earth ion is located in a field consisting of the external field H and the exchange field from the iron subsystem $H_{\text{Fe–R}}$ acting in a perpendicular direction. When the effect of the external field is equal to the magnetizing effect of the exchange field, the terms $(m_{ix}^2 - m_{iy}^2)$ change sign, as a result of which the magnetoelectric polarization (2) also changes sign.

The magnitude of the external magnetic field capable of switching the sign of the magnetoelectric polarization and magnetostriction is determined by the relative magnitude of the Zeeman contribution to the energy of an ion as compared with the Fe–R exchange interaction. The latter is due to the interaction of the spin moments of the rare-earth ions $\mathbf{S}_f$ and the iron ions $\mathbf{S}_{\text{Fe}}$: $I\mathbf{S}_f \cdot \mathbf{S}_{\text{Fe}}$, where I is the exchange integral, which depends on the total moment and the bond angles in the "molecule" $R^{3+}–O^{2-}–Fe^{3+}$. At the same time an external magnetic field acts on the total moment, and its contribution to the energy is determined by the Landé g-factor: $\mu_B g_R J_R H$. The smaller the g-factor, the stronger the external field whose effect equals that of the exchange field is. As is evident from the magnetoelectric dependence for samarium ferroborate (Fig. 14b), polarization switching does not occur up to the strongest external magnetic fields accessible experimentally. The weak action of a magnetic field on the ground state of the Sm multiplet is in good agreement with data obtained from measurements of the magnetic properties of Sm ferroborate (Fig. 7).

E. Spontaneous electric polarization in ferroborates

Below the Néel temperature magnetic ordering induces magnetoelectric polarization, which manifests in fields of the order of 10 kOe with the establishment of antiferromagnetic order in the case of easy-plane ferroborates (Figs. 10 and 14) and in the spin-flop field in easy-axis ferroborates (Fig. 13). However, nonzero electric polarization caused by factors which lower the symmetry of a crystal can be observed in easy-plane samarium ferroborates even in the absence of an external magnetic field (Fig. 3). Such a factor can be uniaxial anisotropy induced by mechanical stresses due to the magnetoelastic interactions.

In compounds where a structural phase transition occurs (R=Ho, Er) the mechanism responsible for spontaneous polarization can be unbalancing, due to mechanical stresses, of the antiferroelectric polarization vectors (Fig. 3). The establishment of magnetic order is accompanied by anomalies in the temperature dependence of the permittivity near the Néel temperature, which dependence differs from the Curie–Weiss law (Fig. 15b). As is well known,[1] multiferroics with extrinsic ferroelectric polarization manifest the strongest magnetoelectric properties.

IV. CONCLUSION

In summary, the presence of spontaneous polarization as well as magnetoelectric and magnetoelastic properties, correlating with one another, makes it possible to classify rare-earth ferroborates $RFe_3(BO_3)_4$ as multiferroics. The ferroelectric ordering arising below T_N is extrinsic. It can be attributed to the lowering of the symmetry of the accompanying the antiferromagnetic ordering as a result of, for example, uniaxial anisotropy induced by internal mechanical stresses in the basal plane, which sets the predominant orientation of the Fe^{3+} spins in a real crystal.

Our studies show a strong dependence not only of the magnetic but also magnetoelectric properties of rare-earth ferroborates on the type of rare-earth ion, specifically, on its anisotropy, which determines the magnetic structure (easy-plane or easy-axis) as well as the considerable contribution to the electric polarization. This is manifested in a strong temperature dependence and increase of the polarization below the Néel point and in its specific field dependence, which manifests most strongly in the cases R=Nd, Sm.

Measurements in strong magnetic fields make it possible to establish a correlation between the magnetoelectric and magnetoelastic properties of rare-earth ferroborates. The magnitude of the magnetoelectric response as compared to the magnetoelastic response is much more sensitive to the ground state of the rare-earth ion. The dielectric anomalies at a structural phase transition, attesting to its antiferroelectric nature, have been explained for the first time.

This work was performed with financial support from RFFI (grant No. 10-02-00848-a).

APPENDIX

To study the electric properties of the system we shall write down, for temperatures below T_s, an invariant (relative to the high-temperature group $R32$) expression for its nonequilibrium thermodynamic potential

$$\Delta\Phi_{el} = \frac{AP^2}{2} + \frac{B}{2}(P_A^2 + P_B^2) + \frac{D}{2}[(\mathbf{P}\cdot\mathbf{P}_A)^2 + (\mathbf{P}\cdot\mathbf{P}_B)^2] + \frac{D'}{4}P^2(P_A^2 + P_B^2) - \mathbf{PE}, \tag{A1}$$

where $\mathbf{P}$ is the electric polarization vector of the system, $(\mathbf{P}_A, \mathbf{P}_B) = q\Delta(\mathbf{n}_1, \mathbf{n}_2)$ are the amplitudes of the transverse wave of polarization (see Eq. (1)) and $\mathbf{E}$ is the external electric field vector; the coefficients A, B, D, D' are thermodynamic parameters of the system.

To determine the equilibrium value of the electric polarization in the system we vary the expression (A1) with respect to the vector $\mathbf{P}$:

$$\frac{\partial\Delta\Phi_{el}}{\partial\mathbf{P}} = 0 = A\mathbf{P} + D[\mathbf{P}_A(\mathbf{P}\cdot\mathbf{P}_A) + \mathbf{P}_B(\mathbf{P}\cdot\mathbf{P}_B)] + \frac{D'}{2}\mathbf{P}[(P_A^2 + P_B^2)] - \mathbf{E}, \tag{A2}$$

We now introduce the vector $\mathbf{n}$, directed along the c axis of the crystal, and we decompose the vector $\mathbf{P}$ along three mutually perpendicular directions parallel to the vectors $\mathbf{n}$, $\mathbf{P}_A$, and $\mathbf{P}_E$:

$$\mathbf{P} = \mathbf{n}(\mathbf{Pn}) + \frac{\mathbf{P}_A}{P_A^2}(\mathbf{P}\cdot\mathbf{P}_A) + \frac{\mathbf{P}_B}{P_B^2}(\mathbf{P}\cdot\mathbf{P}_B). \tag{A3}$$

Then Eq. (A2) takes the form

$$\mathbf{P}(A + D'\Delta^2) + D\Delta^2[\mathbf{P} - (\mathbf{P}\cdot\mathbf{n})\mathbf{n}] = \mathbf{E}. \tag{A4}$$

Hence it follows, specifically, that

$$(\mathbf{P}\cdot\mathbf{n})(A + D'\Delta^2) = (\mathbf{E}\cdot\mathbf{n}). \tag{A5}$$

We shall now represent the solution of the linear vector equation (A5) (whose three projections are a solution of a system of three linear equations) as a sum of components parallel and perpendicular to the $\mathbf{n}$ axis:

$$\mathbf{P} = \kappa_\parallel\mathbf{n}(\mathbf{E}\cdot\mathbf{n}) + \kappa_\perp[\mathbf{E} - \mathbf{n}(\mathbf{E}\cdot\mathbf{n})] \tag{A6}$$

or

$$\mathbf{P} = (\kappa_\parallel - \kappa_\perp)\mathbf{n}(\mathbf{E}\cdot\mathbf{n}) + \kappa_\perp\mathbf{E}. \tag{A7}$$

The quantities $\kappa_\parallel$ and $\kappa_\perp$ are, respectively, the longitudinal and transverse components of the electric susceptibility (polarizability) of the system. Then it follows directly from the relations (A3)–(A5) that

$$\kappa_\parallel = \frac{1}{A + D'\Delta^2}, \quad \kappa_\perp = \frac{1}{A + (D + D')\Delta^2}. \tag{A8}$$

Evidently, the isotropy of the transverse component $\kappa_\perp$ in the basal plane follows from the conditions $P_A^2 = P_B^2 = \Delta^2$, so that the tensor $\kappa_{\alpha\beta}$ will satisfy the following relations: for the diagonal components

$$\kappa_\perp = \kappa_{xx} = \kappa_{yy}, \quad \kappa_\parallel = k_{zz}, \tag{A9}$$

and for the off-diagonal components

$$\kappa_{xy} = \kappa_{yx} = \kappa_{zx} = \kappa_{xz} = \kappa_{yz} = \kappa_{zy} = 0. \tag{A10}$$

We obtain the following relations (in the form of jumps) for the quantities $\kappa_\parallel$ and $\kappa_\perp$ at passing through the structural phase transition point T_s:

$$\Delta\kappa_\parallel = \kappa_\parallel(T = Ts + 0) - \kappa_\parallel(T = T_s - 0) \cong \frac{D'\Delta^2}{A^2} = \kappa(T > T_s)\frac{D'}{A}\Delta^2, \tag{A11a}$$

$$\Delta\kappa_\perp = \kappa_\perp(T = T_s + 0) - \kappa_\perp(T = T_s - 0) \cong \frac{(D + D')\Delta^2}{A^2} = \kappa(T > T_s)\frac{(D + D')}{A}\Delta^2. \tag{A11b}$$

Thus the electric susceptibility of gadolinium ferroborate undergoes a jump at the point T_s of a structural phase transition. The magnitude of this jump is proportional to the squared antiferroelectric order parameter.

[a]Email: kadomts@plms.ru

[1]G. A. Smolenskiĭ and I. E. Chupis, Usp. Fiz. Nauk **137**, 415 (1982) [Sov. Phys. Usp. **25**, 475 (1982)].
[2]Yu. N. Venevtsev, V. V. Gagulin, and V. N. Lyubimov, *Ferroelectric Materials*, Nauka, Moscow (1982).
[3]*Ferroelectric Material, Collection of Works*, edited by Yu. N. Venevtsev and V. N. Lyubimov, Nauka, Moscow (1990).

[4]A. M. Kadomtseva, Yu. F. Popov, A. P. Pyatakov, G. P. Vorob'ev, A. K. Zvezdin, and D. Viehland, Phase Transitions **79**, 1019 (2006).
[5]G. Catalan and J. F. Scott, Adv. Mater. (Weinheim, Ger.) **21**, 2463 (2009).
[6]T. Kimura, T. Goto, H. Shintani, K. Ishiraka, T. Arima, and Y. Tokura, Nature **426**, 55 (2003).
[7]T. Goto, T. Kimura, G. Lawes, A. P. Ramirez, and Y. Tokura, Phys. Rev. Lett. **92**, 257201 (2004).
[8]T. Kimura, G. Lawes, T. Goto, Y. Tokura, and A. P. Ramirez, Phys. Rev. B **71**, 224425 (2005).
[9]V. Yu. Ivanov, A. A. Mukhin, V. D. Travkin, A. S. Prokhorov, Yu. F. Popov, A. M. Kadomtseva, G. P. Vorob'ev, K. I. Kamilov, and A. M. Balbashov, Phys. Status Solidi B **243**, 107 (2006).
[10]J. Hemberger, F. Schrettle, A. Pimenov, P. Lunkenheimer, V. Yu. Ivanov, A. A. Mukhin, A. M. Balbashov, and A. H. Loidl, Phys. Rev. B **75**, 035118 (2007).
[11]A. A. Mukhin, V. Yu. Mukhin, V. Yu. Ivanov, V. D. Travkin, A. S. Prokhorov, A. M. Kadomtseva, Yu. F. Popov, G. P. Vorob'ev, A. V. Pimenov, and A. M. Balbashov, Izv. Ross. Akad. Nauk, Ser. Fiz. **71**, 1658 (2007).
[12]H. Schmid, Ferroelectrics **162**, 317 (1994).
[13]A. K. Zvezdin, S. S. Krotov, A. M. Kadomtseva, G. P. Vorob'ev, Yu. F. Popov, A. P. Pyatakov, L. N. Bezmaternykh, and E. A. Popova, Pis'ma Zh. Eksp. Teor. Fiz. **81**, 335 (2005).
[14]A. K. Zvezdin, G. P. Vorob'ev, A. M. Kadomtseva, Yu. F. Popov, A. P. Pyatakov, L. N. Bezmaternykh, A. V. Kuvardin, and E. A. Popova, Pis'ma Zh. Eksp. Teor. Fiz. **83**, 600 (2006).
[15]A. N. Vasil'ev and E. A. Popova, Fiz. Nizk. Temp. **32**, 968 (2006) [Low Temp. Phys. **32**, 735 (2006)].
[16]M. N. Popova, J. Magn. Magn. Mater. **321**, 716 (2009).
[17]S. A. Klimin, D. Fausti, A. Meetsma, L. N. Bezmaternykh, P. H. M. van Loosdrecht, and T. T. M. Palstra, Acta Crystallogr., Sect. B: Struct. Crystallogr. Cryst. Chem. **61**, 481 (2005).
[18]S. A. Kharlamova, S. G. Ovchinnikov, A. D. Balaev, M. F. Thomas, I. S. Lyubutin, and A. G. Gavriliuk, J. Exp. Theor. Phys. **101**, 1098 (2005).
[19]E. A. Popova, N. Tristan, A. N. Vasiliev, V. L. Temerov, L. N. Bezmaternykh, N. Leps, and B. Bushner, Eur. Phys. J. B **62**, 123 (2008).
[20]R. P. Chaudhury, F. Yen, B. Lorenz, Y. Y. Sun, L. N. Bezmaternykh, V. L. Temerov, and C. W. Chu, Phys. Rev. B **80**, 104424 (2009).
[21]C. Ritter, A. Balaev, A. Vorotynov, G. Petrakovskii, D. Velikanov, V. Temerov, and I. Gudim, J. Phys.: Condens. Matter **19**, 196227 (2007).
[22]C. Ritter, A. Vorontynov, A. Pankrats, G. Petrakovskii, V. Temerov, I. Gudim, and R. Szymczak, J. Phys.: Condens. Matter **20**, 365209 (2008).
[23]P. Fischer, V. Pomjakushin, D. Sheptyakov *et al.*, J. Phys.: Condens. Matter **18**, 7975 (2006).
[24]E. A. Popova, D. V. Volkov, A. N. Vasiliev, A. A. Demidov, N. P. Kolmakova, I. A. Gudim, and L. N. Bezmaternykh, Phys. Rev. B **75**, 224413 (2007).
[25]A. M. Kadomtseva, Yu. F. Popov, G. P. Vorob'ev, A. A. Mukhin, V. Yu. Ivanov, A. M. Kuz'menko, and L. N. Bezmaternykh, Pis'ma Zh. Eksp. Teor. Fiz. **87**, 45 (2008).
[26]E. A. Popova, N. Trisan, H. Hess, R. Klingeler, B. Buekhner, L. N. Bezmaternykh, V. L. Temerov, and A. N. Vasil'ev, Zh. Eksp. Teor. Fiz. **132**, 121 (2007).
[27]D. V. Volkov, A. A. Demidov, and N. P. Kolmakova, Zh. Eksp. Teor. Fiz. **131**, 1030 (2007).
[28]M. N. Popova, E. P. Chukalina, T. N. Stanislavchuk, B. Z. Malkin, A. R. Zakirov, E. Antic-Fidancev, E. A. Popova, L. N. Bezmaternykh, and V. L. Temerov, Phys. Rev. B **75**, 224435 (2007).
[29]M. N. Popova, E. P. Chukalina, T. N. Stanislavchuk, and L. N. Bezmaternykh, J. Magn. Magn. Mater. **300**, e440 (2006).
[30]D. Fausti, A. Nugroho, P. van Loosdrecht, S. A. Klimin, M. N. Popova, and L. N. Bezmaternykh, Phys. Rev. B **74**, 024403 (2006).
[31]M. N. Popova, J. Rare Earths **27**, 607 (2009).
[32]E. A. Туров, Usp. Fiz. Nauk **264**, 325 (1994).
[33]A. I. Pankrats, G. A. Petrakovskiĭ, L. N. Bezmaternykh, and O. A. Bayukov, Zh. Eksp. Teor. Fiz. **126**, 887 (2004).
[34]S. S. Krotov, A. M. Kadomtseva, Yu. F. Popov, G. P. Vorob'ev, A. V. Kuvardin, K. I. Kamilov, L. N. Bezmaternykh, and E. A. Popova, J. Magn. Magn. Mater. **300**, e426 (2006).
[35]M. N. Popova, T. N. Stanislavchuk, B. Z. Malkin, and L. N. Bezmaternykh, Phys. Rev. Lett. **102**, 187403 (2009).
[36]G. A. Zvyagina, K. R. Zhekov, L. N. Bezmaternykh, I. A. Gudim, I. V. Bilych, and A. A. Zvyagin, Fiz. Nizk. Temp. **34**, 1142 (2008) [Low Temp. Phys. **34**, 901 (2008)].
[37]H. Mo, C. S. Nelson, L. N. Bezmaternykh, and V. L. Temerov, Phys. Rev. B **78**, 214407 (2008).

Translated by M. E. Alferieff